Catalysis Today 174 (2011) 17–24

Contents lists available at ScienceDirect

Catalysis Today

journal homepage: www.elsevier.com/locate/cattod

Reaction network and kinetic analysis of ethanol steam reforming over a Ru/Al_2O_3 catalyst

Pei-Jen Lu, Tai-Shang Chen, Jia-Ming Chern*

Department of Chemical Engineering, Tatung University, 40 Chungshan North Road, 3rd Section, Taipei 104, Taiwan

ARTICLE INFO

Article history:
Received 28 October 2010
Received in revised form 3 April 2011
Accepted 13 April 2011
Available online 26 May 2011

Keywords:
Ethanol steam reforming
Hydrogen
Kinetic model
Reaction network

ABSTRACT

Ethanol steam reforming, a potential technology of hydrogen production for fuel cell application, has attracted great research attention recently. Because ethanol can be produced from biomass cheaply, using bioethanol with large excess of water as the direct feed of steam reforming is believed to be a promising technology to produce hydrogen for fuel cells. Although various catalyst systems were used for ethanol steam reforming, detailed reaction kinetics was not investigated thoroughly. In the analysis of heterogeneous catalytic kinetics, reaction mechanism including adsorption step of reactants, reaction step of the adsorbed species, and desorption step of the products were usually proposed. Then a suitable rate determining step was assumed to allow the derivation of the rate equation as a function of reactant and/or product concentrations. In this study, the general rate equations for cyclic reaction networks with multiple pathways were applied to derive the rate equation and hydrogen yield equation for ethanol steam reforming. The derived rate and yield equations were used to analyze the kinetic data of Vaidya and Rodrigues. The results showed that the experimental ethanol conversions and hydrogen yield ratios at varying space times and reaction temperatures could be satisfactorily predicted by the model equations. The rate controlling steps are water reaction with the adsorbed ethanol, water reaction with the adsorbed acetaldehyde, and CO desorption. Furthermore, for temperature lower than 923 K, the overall reaction is also controlled by desorption of ethanol and desorption of acetaldehyde; for temperature higher than 923 K, the overall reaction is also controlled by the dehydrogenation of the adsorbed ethanol. The averaged activation energy of three sequential reaction steps was found to be 110 kJ/mol, compared with the overall activation energy 96 ± 17 kJ/mol determined by Vaidya and Rodrigues.

1. Introduction

Ethanol steam reforming, a potential technology of hydrogen production for fuel cell application, has attracted great research attention recently [1–15]. Because ethanol can be produced from biomass cheaply, using bioethanol with large excess of water as the direct feed of steam reforming is believed to be a promising technology to produce hydrogen for fuel cells [16]. Although various catalyst systems were used for ethanol steam reforming, reaction rate and yield equations were not investigated explicitly [9,16–19]. The desired overall reaction of steam reforming is

$$C_2H_5OH + 3H_2O \rightarrow 2CO_2 + 6H_2 \quad (1)$$

However, if other side reactions are also considered, the reaction network becomes very complicated and thus makes kinetic data analysis very difficult.

Vaidya and Rodrigues studied catalytic steam reforming of ethanol over a $Ru/\gamma\text{-}Al_2O_3$ catalyst in the temperature range 873–973 K and found the ethanol reaction rate was first order with respect to ethanol and independent of water [16]. They proposed a possible reaction mechanism for ethanol steam reforming and derived a rate expression assuming that the decomposition of an activated complex formed during reaction into intermediate products was the rate determining step. Using the derived rate expression and packed-bed reactor model, they obtained an equation to calculate the ethanol conversion as a function of catalyst weight (W) and volumetric feed flow rate (Q_0). Although the equation was used to fit the ethanol conversion versus W/Q_0 data with satisfactory agreement, it cannot be used to interpret other kinetic data such as hydrogen yield.

With the advancement of spectroscopy and other surface analysis techniques, most researches about heterogeneous catalysis focus on catalyst preparation, characterization, and performance tests. Nevertheless, for a given catalyst system an adequate rate equation reflecting the elementary reaction step is very useful for reactor scale-up and process design. In the analysis of heterogeneous catalytic kinetics, reaction mechanism including adsorption

* Corresponding author. Tel.: +886 2 21822928x6277; fax: +886 2 25861939.
E-mail address: jmchern@ttu.edu.tw (J.-M. Chern).

0920-5861/$ – see front matter © 2011 Elsevier B.V. All rights reserved.
doi:10.1016/j.cattod.2011.04.033

step of reactants, reaction step of the adsorbed species, and desorption step of the products were usually proposed. Then a suitable rate determining step was assumed to allow the derivation of the rate equation as a function of reactant and/or product concentrations. Because of complicated reaction steps involved in heterogeneous catalysis, empirical power-law rate equation is usually used. For example, Soyal-Baltacioğlu et al. [9] used a power-law rate equation to analyze the kinetic data of ethanol steam reforming over Pt–Ni catalysts. In this study, the general rate equations for cyclic reaction networks with multiple pathways [20] and pyramidal topology [21] were applied to derive the reaction rate and yield ratio equations for ethanol steam reforming. The derived rate and yield ratio equations were used to analyze the kinetic data of Vaidya and Rodrigues to elucidate how to apply the general rate equations for heterogeneous reaction network analysis.

2. Proposed reaction network

Consider the following main reactions involved in ethanol steam reforming:

$$C_2H_5OH + H_2O \rightarrow CH_4 + CO_2 + 2H_2 \quad (2)$$

$$CH_4 + H_2O \leftrightarrow CO + 3H_2 \quad (3)$$

$$CO + H_2O \leftrightarrow CO_2 + H_2 \quad (4)$$

Reaction (2) is the steam reforming reaction of ethanol that is predominant at these temperatures. Reactions (2)–(4) together denote the overall steam reforming reaction of ethanol. Ethanol dehydrogenation to acetaldehyde and ethanol dehydration to ethylene also occur in the presence of Ru/Al_2O_3 [16]:

$$C_2H_5OH \rightarrow CH_3CHO + H_2 \quad (5)$$

$$C_2H_5OH \rightarrow C_2H_4 + H_2O \quad (6)$$

The formation of ethane observed during ethanol steam reforming may result from ethylene hydrogenation:

$$C_2H_4 + H_2 \rightarrow C_2H_6 \quad (7)$$

The intermediates such as C_2H_4, C_2H_6, and CH_3CHO also possibly undergo steam reforming to produce CO_2 and H_2:

$$C_2H_4 + H_2O \rightarrow CH_4 + CO + H_2 \quad (8)$$

$$C_2H_6 + H_2O \rightarrow CH_4 + CO + 2H_2 \quad (9)$$

$$CH_3CHO + H_2O \rightarrow CH_4 + CO_2 + H_2 \quad (10)$$

The produced CH_4 and CO can be converted to CO_2 and H_2 by Reactions (3) and (4).

The following reaction mechanism is proposed for the above overall reactions:

$$S + C_2H_5OH \underset{k_{10}}{\overset{k_{01}}{\leftrightarrow}} SC_2H_5OH \quad (11)$$

$$SC_2H_5OH + H_2O \xrightarrow{k_{12}} SCH_4 + 2H_2 + CO_2 \quad (12)$$

$$SCH_4 \underset{k_{02}}{\overset{k_{20}}{\leftrightarrow}} S + CH_4 \quad (13)$$

$$SCH_4 + H_2O \xrightarrow{k_{23}} SCO + 3H_2 \quad (14)$$

$$SCO \underset{k_{03}}{\overset{k_{30}}{\leftrightarrow}} S + CO \quad (15)$$

$$SCO + H_2O \xrightarrow{k_{34}} S + H_2 + CO_2 \quad (16)$$

$$SC_2H_5OH \xrightarrow{k'_{12}} SCH_3CHO + H_2 \quad (17)$$

$$SCH_3CHO \underset{k'_{02}}{\overset{k'_{20}}{\leftrightarrow}} S + CH_3CHO \quad (18)$$

$$SCH_3CHO + H_2O \xrightarrow{k'_{23}} SCH_4 + H_2 + CO_2 \quad (19)$$

$$SC_2H_5OH \xrightarrow{k''_{12}} SC_2H_4 + H_2O \quad (20)$$

$$SC_2H_4 \underset{k''_{02}}{\overset{k''_{20}}{\leftrightarrow}} S + C_2H_4 \quad (21)$$

$$SC_2H_4 + H_2 \xrightarrow{k''_{23}} SC_2H_6 \quad (22)$$

$$SC_2H_4 + H_2O \xrightarrow{k''_{24}} SCH_4 + H_2 + CO \quad (23)$$

$$SC_2H_6 \underset{k''_{03}}{\overset{k''_{30}}{\leftrightarrow}} S + C_2H_6 \quad (24)$$

$$SC_2H_6 + H_2O \xrightarrow{k''_{34}} SCH_4 + 2H_2 + CO \quad (25)$$

According to the proposed mechanism, ethanol steam reforming starts with the adsorption of ethanol on the catalyst as shown by Reaction (11). The adsorbed ethanol reacts with water in the gas phase to form the methane-adsorbed species and releases carbon dioxide and hydrogen as shown by Reaction (12). The adsorbed methane can desorb from the catalyst as shown by Reaction (13) or reacts with water in the gas phase to form the CO-adsorbed species and release hydrogen as shown by Reaction (14). The adsorbed CO can desorb from the catalyst as shown by Reaction (15) or reacts with water in the gas phase to release carbon dioxide and hydrogen as shown by Reaction (16).

The adsorbed ethanol can release hydrogen and form the acetaldehyde-adsorbed species as shown by Reaction (17). The adsorbed CH_3CHO can desorb from the catalyst or react with water in the gas phase to release carbon dioxide and hydrogen and form the CH_4-adsorbed species as shown by Reactions (18) and (19), respectively. The adsorbed ethanol can also release water and form the ethylene-adsorbed species as shown by Reaction (20). The adsorbed C_2H_4 can desorb from the catalyst, reacts with hydrogen in the gas phase to form the C_2H_6-adsorbed species or reacts with water in the gas phase to release CO and hydrogen and form the CH_4-adsorbed species as shown by Reactions (21)–(23), respectively. The adsorbed ethane can desorb from the catalyst or react with water in the gas phase to release CO and hydrogen and form the CH_4-adsorbed species as shown by Reactions (24) and (25), respectively.

A reaction network, shown in Fig. 1, can be drawn to show the reaction pathways of the mechanism schematically. As shown in Fig. 1, the overall reactions involved in ethanol steam reforming can be obtained from the following reaction routes with the co-reactants and co-products shown above and below the arrows, respectively:

For Reaction (2),

$$S \overset{C_2H_5OH}{\longleftrightarrow} SC_2H_5OH \underset{2H_2+CO_2}{\overset{H_2O}{\rightarrow}} SCH_4 \underset{CH_4}{\longleftrightarrow} S \quad (26)$$

For Reaction (3),

$$S \overset{CH_4}{\longleftrightarrow} SCH_4 \underset{3H_2}{\overset{H_2O}{\rightarrow}} SCO \underset{CO}{\longleftrightarrow} S \quad (27)$$

For Reaction (4),

$$S \overset{CO}{\longleftrightarrow} SCO \underset{H_2+CO_2}{\overset{H_2O}{\rightarrow}} S \quad (28)$$

For Reaction (5),

$$S \overset{C_2H_5OH}{\longleftrightarrow} SC_2H_5OH \underset{H_2}{\rightarrow} SCH_3CHO \underset{CH_3CHO}{\longleftrightarrow} S \quad (29)$$

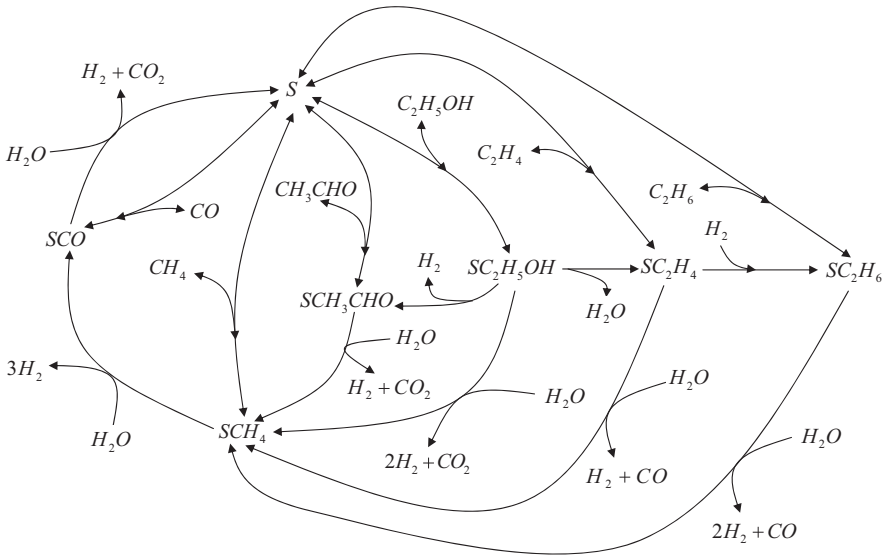

Fig. 1. The reaction network of ethanol steam reforming.

For Reaction (6),

$$S \overset{C_2H_5OH}{\longleftrightarrow} SC_2H_5OH \underset{H_2O}{\longrightarrow} SC_2H_4 \underset{C_2H_4}{\longleftrightarrow} S \tag{30}$$

For Reaction (7),

$$S \overset{C_2H_4}{\longleftrightarrow} SC_2H_4 \overset{H_2}{\longrightarrow} SC_2H_6 \underset{C_2H_6}{\longleftrightarrow} S \tag{31}$$

For Reaction (8),

$$S \overset{C_2H_4}{\longleftrightarrow} SC_2H_4 \underset{H_2+CO}{\overset{H_2O}{\longrightarrow}} SCH_4 \underset{CH_4}{\longleftrightarrow} S \tag{32}$$

For Reaction (9),

$$S \overset{C_2H_6}{\longleftrightarrow} SC_2H_6 \underset{2H_2+CO}{\overset{H_2O}{\longrightarrow}} SCH_4 \underset{CH_4}{\longleftrightarrow} S \tag{33}$$

For Reaction (10),

$$S \overset{CH_3CHO}{\longleftrightarrow} SCH_3CHO \underset{CO_2+H_2}{\overset{H_2O}{\longrightarrow}} SCH_4 \underset{CH_4}{\longleftrightarrow} S \tag{34}$$

3. Reaction rate analysis

Although the proposed reaction mechanism consisting of 15 reaction steps and 21 rate constants is able to describe the possible overall reactions, finding the reaction rates for all the reactants and products is very tedious. Therefore, only the three main reactions and ethanol dehydrogenation shown in Reactions (2)–(5) are considered in analyzing the experimental data of Vaidya and Rodrigues [16]. In the future, if more experimental data of the intermediate products are obtained, the complete reaction network shown in Fig. 1 will be analyzed using the same methodology [20–22].

After neglecting the ethanol dehydration reaction and assuming irreversible desorption of CO, CH_4 and CH_3CHO, the reaction network can be reduced as shown in Fig. 2. The cycle rate and pathway rates shown in Fig. 2 have the following relations: $r = r_1 + r_2$, $r_1 = r_3 + r_4$, $r_2 + r_4 = r_5 + r_6$, $r_6 = r_7 + r_8$. The species reaction rate can be expressed in terms of the overall cycle rate and pathway rates:

$$\begin{aligned} &r_{C_2H_5OH} = -r \quad r_{H_2O} = -r_2 - r_4 - r_6 - r_8 \quad r_{CO_2} = r_2 + r_4 + r_8 \\ &r_{CO} = r_7 \quad\quad r_{CH_4} = r_5 \quad\quad r_{H_2} = r_1 + 2r_2 + r_4 + 3r_6 + r_8 \end{aligned} \tag{35}$$

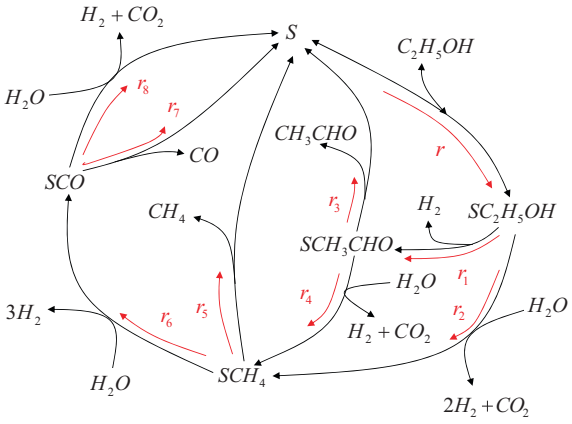

Fig. 2. Reduced reaction network of ethanol steam reforming without considering ethanol dehydration and its related reactions.

3.1. Cycle rate and pathway reaction rates

The reaction network shown in Fig. 2 contains multiple pathways between some intermediates. With successive grouping the multiple pathways, the overall cycle rate can be obtained. At first,

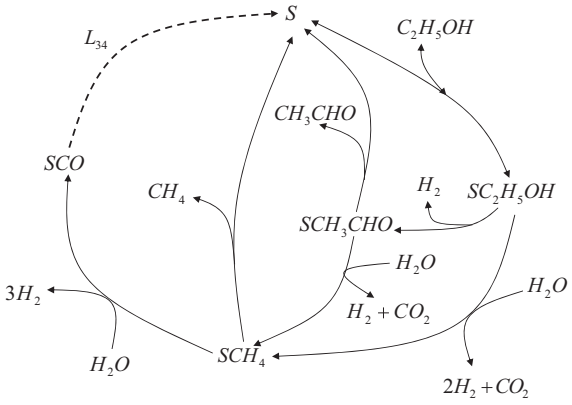

Fig. 3. Modified reaction network of ethanol steam reforming after grouping the pathways between SCO site and S site.

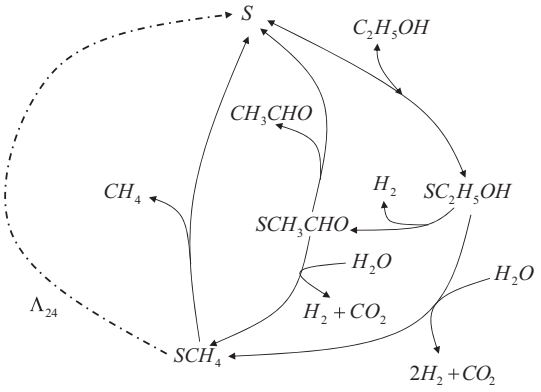

Fig. 4. Modified reaction network of ethanol steam reforming after eliminating the SCO site.

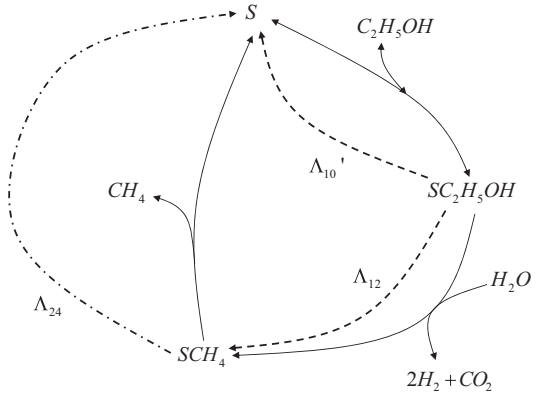

Fig. 5. Modified reaction network of ethanol steam reforming after Y-to-delta transformation.

the two pathways between the CO-adsorbed site, SCO, and the free catalyst site, S, are grouped as a single step with the loop rate coefficient $L_{34} = k_{34}C_W + k_{30}$ [21]. After this grouping, the equivalent reaction network is modified and shown in Fig. 3. Moreover the pathway $SCH_4 \rightarrow SCO \rightarrow S$ can be reduced to a single step $SCH_4 \rightarrow S$ by the network reduction technique [22] with the reduced step rate coefficient, $\Lambda_{24} = k_{23}C_W$. After eliminating the SCO intermediate, the reaction network can be further modified as one shown in Fig. 4. Apply the Y-to-delta transformation technique [21], the reaction network shown in Fig. 4 can be reduced to that shown in Fig. 5 with the Λ coefficients $\Lambda'_{10} = k'_{12}k'_{20}/(k'_{20} + k'_{23}C_W)$ and $\Lambda_{12} = k'_{12}k'_{23}C_W/(k'_{20} + k'_{23}C_W)$. Finally, the two pathways between S, SC_2H_5OH, and SCH_4 can be combined respectively to convert the reaction network to a single cycle network as shown in Fig. 6. The loop coefficients shown in Fig. 6 are $L_{20} = k_{20} + \Lambda_{24}$, $L_{12} = k_{12}C_W + \Lambda_{12}$, $L_{10} = k_{10} + \Lambda'_{10}$, and $L_{01} = k_{01}C_E$ where C_E is the ethanol concentration.

The rate equation of the single cycle network, equal to $r_5 + r_6$, can be expressed by the following equation [22]:

$$r_5 + r_6 = \frac{L_{01}L_{12}L_{20}C_{ST}}{D_{00} + D_{11} + D_{22} + (k'_{12}/(k'_{20} + k'_{23}C_W))D_{11} + (k_{23}C_W/L_{34})D_{22}} \quad (36)$$

where C_{ST} is the total catalyst concentration. In Eq. (36), the last two terms of the denominator are included to account for the missed SCH_3CHO and SCO intermediates due to network reduction [20].

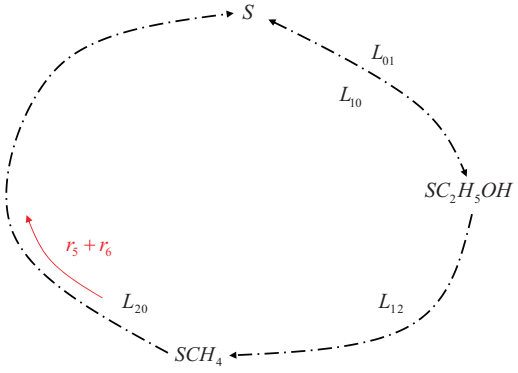

Fig. 6. Reduced single-cycle reaction network of ethanol steam reforming.

From Eq. (36), the intermediate SCH_4 concentration can be obtained and the pathway rates for r_5 and r_6 can thus be calculated by the following equations:

$$\begin{cases} r_5 = \dfrac{L_{01}L_{12}k_{20}C_{ST}}{D_{00} + D_{11} + D_{22} + (k'_{12}/(k'_{20} + k'_{23}C_W))D_{11} + (k_{23}C_W/L_{34})D_{22}} \\ r_6 = \dfrac{L_{01}L_{12}k_{23}C_WC_{ST}}{D_{00} + D_{11} + D_{22} + (k'_{12}/(k'_{20} + k'_{23}C_W))D_{11} + (k_{23}C_W/L_{34})D_{22}} \end{cases} \quad (37)$$

Using Eq. (37) and the relations of $r_7/r_8 = k_{30}/(k_{34}C_W)$ and $r_7 + r_8 = r_6$, the pathway rates for r_7 and r_8 can be calculated by the following equations:

$$\begin{cases} r_7 = \dfrac{k_{30}}{k_{30} + k_{34}C_W} \dfrac{L_{01}L_{12}k_{23}C_WC_{ST}}{D_{00} + D_{11} + D_{22} + (k'_{12}/(k'_{20} + k'_{23}C_W))D_{11} + (k_{23}C_W/L_{34})D_{22}} \\ r_8 = \dfrac{k_{34}C_W}{k_{30} + k_{34}C_W} \dfrac{L_{01}L_{12}k_{23}C_WC_{ST}}{D_{00} + D_{11} + D_{22} + (k'_{12}/(k'_{20} + k'_{23}C_W))D_{11} + (k_{23}C_W/L_{34})D_{22}} \end{cases} \quad (38)$$

From Eq. (36), the intermediate SC_2H_5OH concentration can be obtained and the pathway rates for r_1 and r_2 can thus be calculated by the following equations:

$$\begin{cases} r_1 = \dfrac{L_{01}k'_{12}L_{20}C_{ST}}{D_{00} + D_{11} + D_{22} + (k'_{12}/(k'_{20} + k'_{23}C_W))D_{11} + (k_{23}C_W/L_{34})D_{22}} \\ r_2 = \dfrac{L_{01}k_{12}L_{20}C_WC_{ST}}{D_{00} + D_{11} + D_{22} + (k'_{12}/(k'_{20} + k'_{23}C_W))D_{11} + (k_{23}C_W/L_{34})D_{22}} \end{cases} \quad (39)$$

During the Y-to-delta transformation, the concentration of the missed intermediate SCH_3CHO can be expressed in terms of the intermediate SC_2H_5OH concentration, so that the pathway rates for r_3 and r_4 can thus be calculated by the following equations:

$$\begin{cases} r_3 = \dfrac{k'_{12}}{k'_{20} + k'_{23}C_W} \dfrac{L_{01}k_{20}k'_{20}C_{ST}}{D_{00} + D_{11} + D_{22} + (k'_{12}/(k'_{20} + k'_{23}C_W))D_{11} + (k_{23}C_W/L_{34})D_{22}} \\ r_4 = \dfrac{k'_{12}}{k'_{20} + k'_{23}C_W} \dfrac{L_{01}L_{20}k'_{24}C_WC_{ST}}{D_{00} + D_{11} + D_{22} + (k'_{12}/(k'_{20} + k'_{23}C_W))D_{11} + (k_{23}C_W/L_{34})D_{22}} \end{cases} \quad (40)$$

The D_{ii} terms in the denominator of Eqs. (36)–(40) can be evaluated by using the Helfferich formula [20] to consider the following linear pathways:

$$D_{00} = L_{12}L_{20} + L_{10}L_{20} \quad \text{for } S \underset{L_{10}}{\overset{L_{01}}{\leftrightarrow}} SC_2H_5OH \xrightarrow{L_{12}} SCH_4 \xrightarrow{L_{20}} S \quad (41)$$

$$D_{11} = L_{01}L_{20} \quad \text{for } SC_2H_5OH \xrightarrow{L_{12}} SCH_4 \xrightarrow{L_{20}} S \underset{L_{10}}{\overset{L_{01}}{\leftrightarrow}} SC_2H_5OH \quad (42)$$

$$D_{22} = L_{01}L_{12} \quad \text{for } SCH_4 \xrightarrow{L_{20}} S \underset{L_{10}}{\overset{L_{01}}{\leftrightarrow}} SC_2H_5OH \xrightarrow{L_{12}} SCH_4 \quad (43)$$

Substituting all the D_{ii} terms into all the pathway rate equations and replacing the Λ coefficients and loop coefficients by the rate

constants leads to

$$r_1 = \frac{k_{01}k'_{12}(k_{20}+k_{23}C_W)(k'_{20}+k'_{23}C_W)(k_{34}C_W+k_{30})C_{ST}C_E}{D} \quad (44)$$

$$r_2 = \frac{k_{01}k_{12}(k_{20}+k_{23}C_W)(k'_{20}+k'_{23}C_W)(k_{34}C_W+k_{30})C_{ST}C_WC_E}{D} \quad (45)$$

$$r_3 = \frac{k_{01}k'_{12}k'_{20}k'_{20}(k_{34}C_W+k_{30})C_{ST}C_E}{D} \quad (46)$$

$$r_4 = \frac{k_{01}k'_{12}k'_{24}(k_{20}+k_{23}C_W)(k_{34}C_W+k_{30})C_WC_{ST}C_E}{D} \quad (47)$$

$$r_5 = \frac{k_{01}k_{20}(k_{12}k'_{20}+k_{12}k'_{23}C_W+k'_{12}k'_{23})(k_{34}C_W+k_{30})C_{ST}C_WC_E}{D} \quad (48)$$

$$r_6 = \frac{k_{01}k_{23}(k_{12}k'_{20}+k_{12}k'_{23}C_W+k'_{12}k'_{23})(k_{34}C_W+k_{30})C_{ST}C_W^2C_E}{D} \quad (49)$$

$$r_7 = \frac{k_{01}k_{23}k_{30}(k_{12}k'_{20}+k_{12}k'_{23}C_W+k'_{12}k'_{23})C_{ST}C_W^2C_E}{D} \quad (50)$$

$$r_8 = \frac{k_{01}k_{23}k_{34}(k_{12}k'_{20}+k_{12}k'_{23}C_W+k'_{12}k'_{23})C_{ST}C_W^3C_E}{D} \quad (51)$$

where

$$\begin{aligned} D = {} & (k'_{20}k_{12}+k'_{23}k_{12}C_W+k'_{12}k'_{23})(k_{20}+k_{23}C_W)(k_{34}C_W+k_{30})C_W \\ & +(k_{10}k'_{20}+k_{10}k'_{23}C_W+k'_{12}k'_{20})(k_{20}+k_{23}C_W)(k_{34}C_W+k_{30}) \\ & +k_{01}(k_{20}+k_{23}C_W)(k'_{20}+k'_{23}C_W)(k_{34}C_W+k_{30})C_E \\ & +k_{01}(k'_{20}k_{12}+k'_{23}k_{12}C_W+k'_{12}k'_{23})(k_{34}C_W+k_{30})C_WC_E \\ & +k'_{12}k_{01}(k_{20}+k_{23}C_W)(k_{34}C_W+k_{30})C_E \\ & +k_{23}k_{01}(k'_{20}k_{12}+k'_{23}k_{12}C_W+k'_{12}k'_{23})C_W^2C_E \end{aligned} \quad (52)$$

Substituting Eqs. (44) to (51) into Eq. (35), the rate equations of the reactants and products can be calculated. Since the hydrogen yield data were given by Vaidya and Rodrigues, the hydrogen yield ratio equation is investigated in more detail.

3.2. Yield ratio

Because hydrogen generation is the desired product of primary interest, we can define the hydrogen yield ratio as:

$$Y_{H_2} \equiv \frac{r_{H_2}}{-6r_{C_2H_5OH}} = \frac{r_1+2r_2+r_4+3r_6+r_8}{6r} \quad (53)$$

Substituting the pathway rates into Eq. (53) leads to

$$\begin{aligned} Y_{H_2} = {} & \frac{k'_{12}}{6(k'_{12}+k_{12}C_W)} + \frac{k_{12}C_W}{3(k'_{12}+k_{12}C_W)} \\ & + \frac{k'_{12}k'_{23}C_W}{6(k'_{12}+k_{12}C_W)(k'_{20}+k'_{23}C_W)} \\ & + \frac{k_{23}C_W^2(k_{12}k'_{20}+k'_{12}k'_{23}+k'_{12}k'_{23}C_W)}{2(k'_{12}+k_{12}C_W)(k_{20}+k_{23}C_W)(k'_{12}+k'_{12}C_W)} \\ & + \frac{k_{23}k_{34}C_W^3(k_{12}k'_{20}+k'_{12}k'_{23}+k_{12}k'_{23}C_W)}{6(k'_{12}+k_{12}C_W)(k_{20}+k_{23}C_W)(k'_{20}+k'_{23}C_W)(k_{34}C_W+k_{30})} \end{aligned} \quad (54)$$

4. Comparison with experimental data

Vaidya and Rodrigues packed commercial Ru/γ-Al_2O_3 catalyst in a fixed-bed down-flow reactor placed inside a temperature-controlled heating furnace to carry out ethanol steam reforming.

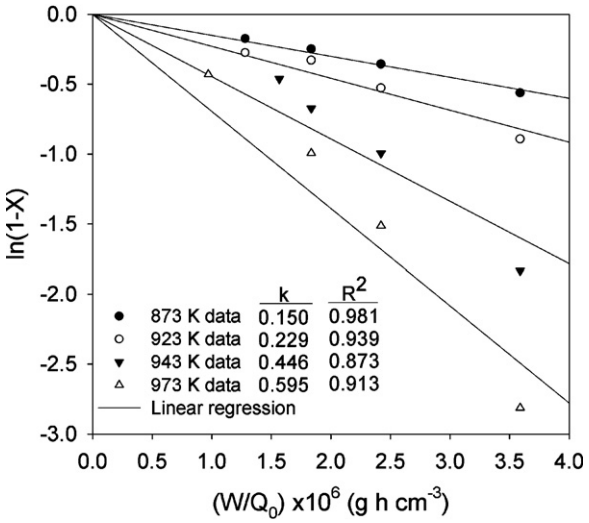

Fig. 7. Linearized plots for the first-order kinetic model.

The liquid feed consisting of an ethanol–water mixture was evaporated and mixed with nitrogen before entering the catalyst bed. All experiments were conducted at atmospheric pressure and isothermally at 4 different temperatures, 873 K, 923 K, 943 K, and 973 K.

Vaidya and Rodrigues used the following first-order kinetics model to analyze their data:

$$\ln(1-X) = -k\frac{W}{Q_0} \quad (55)$$

The $\ln(1-X)$ versus W/Q_0 plots at higher temperatures being not good straight lines as shown in Fig. 7 suggest the first-order kinetics model is not proper to describe the kinetics of ethanol steam reforming at all temperatures.

Since the feed mole ratio of water to ethanol used by Vaidya and Rodrigues is 10–1, the water vapor concentration can be reasonably assumed to be constant during reaction. Thus, the ethanol reaction rate, r_1+r_2 becomes

$$-r_E = \frac{k_{01}(k'_{12}+k_{12}C_{W0})(k_{20}+k_{23}C_{W0})(k'_{20}+k'_{23}C_{W0})(k_{34}C_{W0}+k_{30})C_{ST}C_E}{\Delta} \quad (56)$$

with the denominator

$$\begin{aligned} \Delta = {} & (k'_{20}k_{12}+k'_{23}k_{12}C_{W0}+k'_{12}k'_{23})(k_{20}+k_{23}C_{W0})(k_{34}C_{W0}+k_{30})C_{W0} \\ & +(k_{10}k'_{20}+k_{10}k'_{23}C_{W0}+k'_{12}k'_{20})(k_{20}+k_{23}C_{W0})(k_{34}C_{W0}+k_{30}) \\ & +k_{01}(k_{20}+k_{23}C_{W0})(k'_{20}+k'_{23}C_{W0})(k_{34}C_{W0}+k_{30})C_E \\ & +k_{01}(k'_{20}k_{12}+k'_{23}k_{12}C_{W0}+k'_{12}k'_{23})(k_{34}C_{W0}+k_{30})C_{W0}C_E \\ & +k'_{12}k_{01}(k_{20}+k_{23}C_{W0})(k_{34}C_{W0}+k_{30})C_E \\ & +k_{23}k_{01}(k'_{20}k_{12}+k'_{23}k_{12}C_{W0}+k'_{12}k'_{23})C_{W0}^2C_E \end{aligned} \quad (57)$$

where C_{W0} is the feed water concentration.

Eq. (56), consisting of 10 rate constants and one total catalyst concentration, is the rate equation for ethanol in the presence of excess water without assuming any determining step. Because there are only 4 data points at the same reaction temperature, the 11 parameters in Eqs. (56) and (57) cannot be determined separately. Only some lumped parameters can be obtained. Eq. (56) can be rewritten as

$$-r_E = \frac{k_aC_E}{1+k_bC_E} \quad (58)$$

with the lumped parameters defined as:

$$k_a = \frac{k_{01}(k'_{12}+k_{12}C_{W0})(k'_{20}+k'_{23}C_{W0})C_{ST}}{k'_{20}(k_{10}+k'_{12})+(k_{12}k'_{20}+k'_{12}k'_{23}+k_{10}k'_{23})C_{W0}+k_{12}k'_{23}C_{W0}^2} \quad (59)$$

$$k_b = k_{01}\frac{(k'_{12}+k'_{20}+k'_{23}C_{W0})(k_{20}+k_{23}C_{W0})(k_{34}C_{W0}+k_{30})+(k_{34}C_{W0}^2+k_{30}C_{W0}+k_{23}C_{W0}^2)(k'_{20}k_{12}+k'_{23}k_{12}C_{W0}+k'_{12}k'_{23})}{(k_{10}k'_{20}+k'_{12}k'_{20}+k_{10}k'_{23}C_{W0}+k'_{20}k_{12}C_{W0}+k'_{12}k'_{23}C_{W0}+k'_{23}k_{12}C_{W0}^2)(k_{20}+k_{23}C_{W0})(k_{34}C_{W0}+k_{30})} \quad (60)$$

During each test at given temperature and feed water concentration, k_a and k_b are constant. The rate equation for packed bed reactor operated at steady state is

$$\frac{dF_E}{dW} = r_E = -\frac{k_a C_E}{1 + k_b C_E} \tag{61}$$

where F_E is the molar flow rate of ethanol, W is the packed catalyst weight. The ethanol molar flow rate is related to the ethanol conversion: $F_E = F_{E0}(1 - X)$. The ethanol concentration can be expressed in terms of the volumetric flow rate that was kept constant in the experiments of Vaidya and Rodrigues:

$$C_E = \frac{F_E}{Q} = \frac{F_{E0}(1 - X)}{Q_0} = C_{E0}(1 - X) \tag{62}$$

where Q_0 is the volumetric feed flow rate and C_{E0} is the ethanol feed concentration.

Combining Eqs. (61) and (62) leads to

$$F_{E0}\frac{dX}{dW} = \frac{k_a C_{W0} C_{E0}(1 - X)}{1 + k_b C_{E0}(1 - X)} \tag{63}$$

Eq. (63) can be integrated using boundary condition, at $W = 0, X = 0$, to obtain

$$\frac{k_b C_{E0}}{k_a C_{W0}} X - \frac{1}{k_a C_{W0}} \ln(1 - X) = \frac{C_{E0} W}{F_{E0}} = \frac{W}{Q_0} \tag{64}$$

In Eq. (64), the feed water concentration, C_{W0}, is equal to the feed water mole fraction multiplying the total feed concentration that can be calculated by P/RT. Although Eq. (64) can be used to analyze the steady-state ethanol conversion as a function of W/Q_0, it cannot be used to compare the data of different test runs with different feed water concentrations unless the lumped parameters k_a and k_b at different feed water concentrations are assumed to be constant or can be simplified. Consider parameter k_a first:

If the ethanol dehydration rate is much faster than the ethanol steam reforming rate,

$$\lim_{k'_{12} \gg k_{12} C_{W0}} k_a = \frac{k_{01} k'_{12} C_{ST}}{k_{10} + k'_{12}} \tag{65}$$

If the ethanol dehydration rate is much slower than the ethanol steam reforming rate,

$$\lim_{k'_{12} \ll k_{12} C_{W0}} k_a = \frac{k_{01} k_{12} C_{W0} C_{ST}}{k_{10} + k_{12} C_{W0}} \tag{66}$$

In these two cases, the lumped parameter k_a can be simplified. Before considering the lumped parameter k_b, the hydrogen yield ratio is considered first:

$$\lim_{k'_{12} \gg k_{12} C_{W0}} Y_{H_2} = \frac{1}{6} + \frac{k'_{23} C_{W0}}{6(k'_{20} + k'_{23} C_{W0})} + \frac{k_{23} C_{W0}^2 (k_{12} k'_{20} + k'_{12} k'_{23})}{2k'_{12}(k_{20} + k_{23} C_{W0})(k'_{20} + k'_{23} C_{W0})} + \frac{k_{23} k_{34} C_{W0}^3 (k_{12} k'_{20} + k'_{12} k'_{23})}{6k'_{12}(k_{20} + k_{23} C_{W0})(k'_{20} + k'_{23} C_{W0})(k_{34} C_{W0} + k_{30})} \tag{67}$$

$$\lim_{k'_{12} \ll k_{12} C_{W0}} Y_{H_2} = \frac{1}{3} + \frac{k'_{12} k'_{23} C_{W0}}{6k_{12} C_{W0}(k'_{20} + k'_{23} C_{W0})} + \frac{k_{23} C_{W0}^2}{2C_{W0}(k_{20} + k_{23} C_{W0})} + \frac{k_{23} k_{34} C_{W0}^2}{6(k_{20} + k_{23} C_{W0})(k_{34} C_{W0} + k_{30})} \tag{68}$$

The hydrogen yield ratio, being greater than 1/3 as shown in Eq. (68), does not agree with the data of Vaidya and Rodrigues. This indicates that the ethanol dehydration rate cannot be much slower than the ethanol steam reforming rate. Eqs. (65) and (67) will therefore be applied for data analysis. k_b/k_a is further considered:

$$\lim_{k'_{12} \gg k_{12} C_{W0}} \frac{k_b}{k_a} = \frac{1}{C_{ST}(k'_{20} + k'_{23} C_{W0})} + \frac{1}{C_{ST} k'_{12}} + \frac{C_{W0}(k'_{20} k'_{12} + k'_{12} k'_{23})}{C_{ST} k'_{12}(k'_{20} + k'_{23} C_{W0})(k_{20} + k_{23} C_{W0})} + \frac{C_{W0} k_{30}(k'_{20} k_{12} + k'_{12} k'_{23})}{C_{ST} k'_{12}(k'_{20} + k'_{23} C_{W0})(k_{20} + k_{23} C_{W0})(k_{34} C_{W0} + k_{30})} \tag{69}$$

To simplify Eq. (69), let us reasonably assume that ethanol steam reforming rate is much slower than the CH_3CHO and CO desorption rate, i.e., $k'_{20} \gg k'_{23} C_{W0}$, and $k_{30} \ll k_{34} C_{W0}$.

$$\lim_{\substack{k'_{12} \gg k_{12} C_{W0} \\ k'_{20} \gg k'_{23} C_{W0} \\ k_{30} \gg k_{34} C_{W0}}} \frac{k_b}{k_a} = \frac{k'_{12} + k'_{20}}{C_{ST} k'_{12} k'_{20}} \tag{70}$$

Substituting Eqs. (65) and (70) into Eq. (64) leads to

$$\frac{W}{Q_0} = \left[\frac{k'_{12} + k'_{20}}{k'_{12} k'_{20} C_{ST}}\right] y_{E0} X - \frac{k_{10} + k'_{12}}{k_{01} k'_{12} C_{ST}} \frac{\ln(1 - X)}{C_{W0}} \tag{71}$$

where y_{E0} is the ethanol to water feed ratio. Eq. (71) with two independent parameters $k'_{12} + k'_{20}/k'_{12} k'_{20} C_{ST}$ and $k_{10} + k'_{12}/k_{01} k'_{12} C_{ST}$ is then used to correlate the experimental conversion data shown in Table 1. Assuming $k'_{20} \gg k'_{23} C_{W0}$, and $k_{30} \ll k_{34} C_{W0}$ also leads to

$$\lim_{\substack{k'_{12} \gg k_{12} C_{W0} \\ k'_{20} \gg k'_{23} C_{W0} \\ k_{30} \gg k_{34} C_{W0}}} Y_{H_2} = \frac{1}{6} + \frac{k_{23} k'_{23} C_{W0}^2}{2k'_{20} k_{20}} \tag{72}$$

It is important to note that the hydrogen yield ratio will be greater than 1/3 if $k'_{20} \ll k'_{23} C_{W0}$ or $k_{30} \ll k_{34} C_{W0}$. Eq. (72) can be rewritten as:

$$Y_{H_2} = \frac{1}{6} + \frac{A_{23} A'_{23}}{2A'_{20} A_{20}} \exp\left[-\frac{E_{23} + E'_{23} - E'_{20} - E_{20}}{RT}\right] C_{W0}^2 \tag{73}$$

In Eq. (73), the feed water concentration, C_{W0}, is equal to the feed water mole fraction multiplying the total feed concentration that can be calculated by P/RT. Eq. (73) with 2 parameters

Table 1
The experimental results of Vaidya and Rodrigues.

Y_{E0}	y_{W0}	Q_0 (cm^3 min^{-1})	W/F_{E0} (g h mol^{-1})	T (K)	X	X^a	X^b
0.043	0.43	246.1	2.04	873	0.43	0.42	0.43
0.058	0.58	362.9	1.02	873	0.30	0.30	0.30
0.066	0.66	479.7	0.68	873	0.22	0.24	0.23
0.058	0.58	362.9	0.54	873	0.16	0.17	0.16
0.043	0.43	246.1	2.04	923	0.59	0.56	0.59
0.058	0.58	362.9	1.02	923	0.41	0.43	0.40
0.066	0.66	479.7	0.68	923	0.28	0.34	0.31
0.058	0.58	362.9	0.54	923	0.24	0.25	0.21
0.043	0.43	246.1	2.04	943	0.84	0.80	0.84
0.058	0.58	362.9	1.02	943	0.63	0.66	0.61
0.066	0.66	479.7	0.68	943	0.49	0.56	0.48
0.071	0.71	595.7	0.54	943	0.37	0.50	0.41
0.043	0.43	246.1	2.04	973	0.94	0.92	0.94
0.058	0.58	362.9	1.02	973	0.78	0.81	0.78
0.066	0.66	479.7	0.68	973	0.63	0.72	0.63
0.066	0.66	479.7	0.36	973	0.35	0.49	0.35

[a] Ethanol conversion calculated by the first-order kinetics model.
[b] Ethanol conversion calculated by Eq. (71).

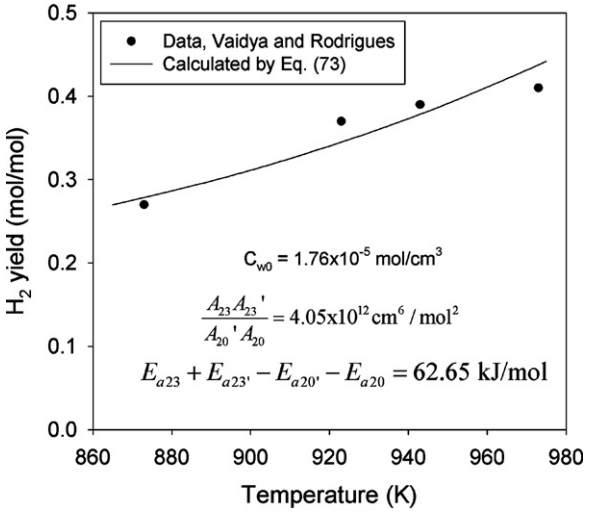

Fig. 8. Experimental and predicted hydrogen yields at varying temperatures.

Table 2
Values of the lumped parameters at various temperatures.

T (K)	$k'_{12} + k'_{20}/k'_{12}k'_{20}C_{ST}$ (g h cm^{-3})	$k_{10} + k'_{12}/k_{01}k'_{12}C_{ST}$ (g h mol cm^{-6})
873	7.86×10^{-5}	6.25×10^{-12}
923	5.90×10^{-5}	1.87×10^{-12}
943	3.60×10^{-5}	5.23×10^{-12}
973	2.43×10^{-5}	8.14×10^{-12}

$A_{23}A'_{23}/A'_{20}A_{20}$ and $E_{23} + E'_{23} - E'_{20} - E_{20}$ is used to correlate the experimental hydrogen yield ratio data at different temperatures.

Fig. 8 shows the experimental hydrogen yield ratios at different temperatures and those calculated by Eq. (73) using the parameters determined from a linear plot of $Y_{H_2} - 1/6$ versus $1/T$. The lumped parameters obtained from the linear plot are: $A_{23}A'_{23}/A'_{20}A_{20} = 4.05 \times 10^{12}$ cm^6/mol^2 and $E_{23} + E'_{23} - E'_{20} - E_{20} = 62.65$ kJ/mol. As is shown in Fig. 8, the proposed kinetic model predicts the hydrogen yield ratios satisfactorily.

The two lumped parameters in Eq. (71) at different temperatures, determined from nonlinear regression of the experimental ethanol conversion data are listed in Table 2. Using the two lumped parameters and Eq. (71), the ethanol conversion at different feed water concentrations and temperatures can be calculated and shown in Table 1. As is shown in Table 1, the average absolute errors calculated by AAE $= (1/N)\sum_{i=1}^{N}|X_{\text{exp},i} - X_{cal'd,i}/X_{\text{exp},i}|$ for the first-order model and Eq. (71) are 10.78% and 2.89%, respectively. Obviously, the kinetic model equation derived from our proposed reaction mechanism gives better fit to the experimental ethanol conversions at different feed water concentrations and temperatures.

Only the lumped parameters in Eq. (71) at different temperatures can be obtained from nonlinear regression of the experimental data. However, some individual rate constants can be determined from the Arrhenius plots of the lumped parameters as shown in Fig. 9b and c, respectively. The significant change of the slope at $T = 923$ K in Fig. 9c suggests that $k_{10} \ll k'_{12}$ for $T \leq 923$ K. In this case, $k_{10} + k'_{12}/k_{01}k'_{12}C_{ST} \approx 1/k_{01}C_{ST} = e^{E_{01}/RT}/A_{01}C_{ST}$, the activation energy of ethanol adsorption and the pre-exponential constant determined from the Arrhenius plot are: $E_{01} = 162.0$ kJ/mol and $A_{01}C_{ST} = 7.84 \times 10^{20}$ cm^6 g^{-1} h^{-1} mol^{-1}, respectively. We can also reasonably assume $k_{10} \gg k'_{12}$ for $T \geq 923$ K that leads to $k_{10} + k'_{12}/k_{01}k'_{12}C_{ST} \approx k_{10}/k_{01}k'_{12}C_{ST} = A_{10}e^{(E'_{12}+E_{01}-E_{10})/RT}/A_{01}A'_{12}C_{ST}$. The lumped activation energy and the pre-exponential constant determined from the Arrhenius plot are: $E'_{12} + E_{01} - E_{10} = -212.5$ kJ/mol and $A_{10}/A_{01}A'_{12}C_{ST} = 2.348$ g h cm^{-3}, respectively.

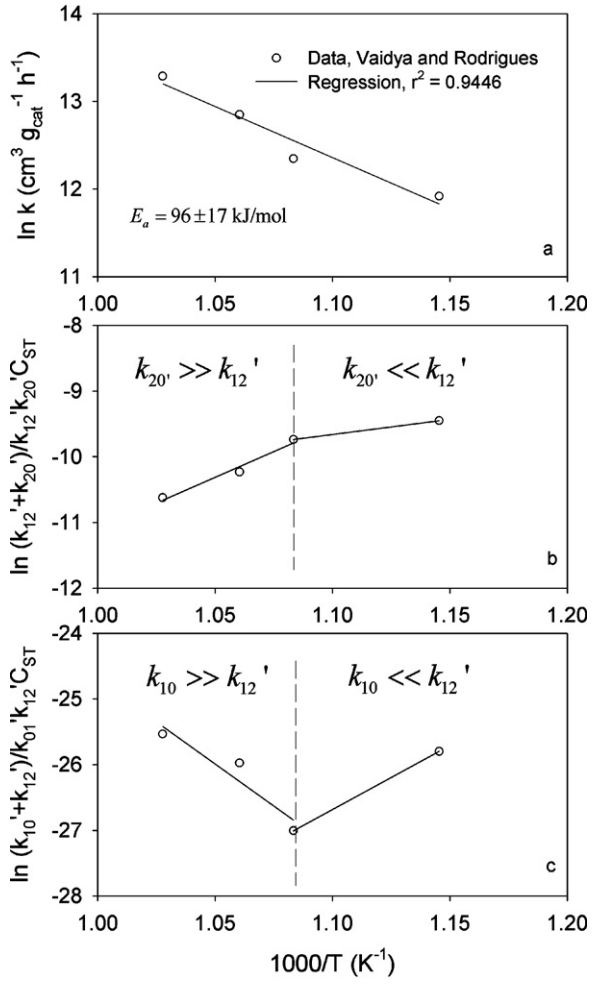

Fig. 9. Arrhenius plot for the rate constants.

For $T \leq 923$ K, we can also reasonably assume $k'_{20} \ll k'_{12}$ and get $k'_{12} + k'_{20}/k'_{12}k'_{20}C_{ST} \approx 1/k'_{20}C_{ST} = e^{E_{20'}/RT}/A'_{20}C_{ST}$. The activation energy of acetaldehyde desorption and the pre-exponential constant determined from the Arrhenius plot are: $E'_{20} = 38.5$ kJ/mol and $A'_{20}C_{ST} = 2.57 \times 10^6$ cm^3 g^{-1} h^{-1}, respectively. Similarly, assuming $k'_{20} >> k'_{12}$ for $T \geq 923$ K leads to $k'_{12} + k'_{20}/k'_{12}k'_{20}C_{ST} \approx 1/k'_{12}C_{ST} = e^{E'_{12}/RT}/A'_{12}C_{ST}$. The activation energy of ethanol dehydrogenation and the pre-exponential constant determined from the Arrhenius plot are: $E'_{12} = 130.0$ kJ/mol and $A'_{12}C_{ST} = 4.08 \times 10^{11}$ cm^3 g^{-1} h^{-1}, respectively.

5. Summary of kinetic models

It is not necessary to assume any rate determining step to derive the rate equation of ethanol steam reforming. In fact, no single rate determining step can be assumed to obtain the rate equation that reasonably fit the experimental data. However, some reaction steps with smaller rate constants should be the important steps controlling the overall rate. According to the analysis of the hydrogen yield and ethanol conversion data, the following important rate controlling steps can be identified:

$k'_{12} \gg k_{12}C_{W0}$ indicates that $SC_2H_5OH + H_2O \xrightarrow{k_{12}} SCH_4 + 2H_2 + CO_2$ step is important.

$k'_{20} \gg k'_{23}C_{W0}$ indicates that $SCH_3CHO + H_2O \xrightarrow{k'_{23}} SCH_4 + H_2 + CO_2$ step is important.

$k_{30} \ll k_{34}C_{W0}$ indicates that $SCO \xrightarrow{k_{30}} S + CO$ step is important.

For $T \leq 923$ K,

$k_{10} \ll k'_{12}$ and $k'_{20} \ll k'_{12}$ indicate that $SC_2H_5OH \xrightarrow{k_{10}} S + C_2H_5OH$ step and $SCH_3CHO \xrightarrow{k'_{20}} S + CH_3CHO$ step are important.

For $T \geq 923$ K,

$k_{10} \gg k'_{12}$ and $k'_{20} \gg k'_{12}$ indicate that $SC_2H_5OH \xrightarrow{k'_{12}} SCH_3CHO + H_2$ step is important.

According to the above analysis, the hydrogen yield ratio is related to the feed water concentration and reaction temperature by the following equation:

$$Y_{H_2} = \frac{1}{6} + 2.02 \times 10^{12} \exp\left[-\frac{7535}{T}\right] C_{W0}^2 \tag{74}$$

with the unit T in K and C_{W0} in mol/cm^3.

The ethanol conversion is related to the space time, feed ethanol mole fraction, feed water concentration and reaction temperature by the following equation:

$$\begin{cases} \dfrac{W}{Q_0} = \dfrac{e^{4635/T}}{2.57 \times 10^6} y_{E0} X - \dfrac{e^{19479/T}}{7.84 \times 10^{20}} \dfrac{\ln(1-X)}{C_{W0}} & T \leq 923\,\text{K} \\ \dfrac{W}{Q_0} = \dfrac{e^{15642/T}}{4.08 \times 10^{11}} y_{E0} X - \dfrac{e^{-25564/T}}{2.348} \dfrac{\ln(1-X)}{C_{W0}} & T \geq 923\,\text{K} \end{cases} \tag{75}$$

with the unit W/Q_0 in g h/cm^3.

The activation energies of three reaction steps can be determined:

- Adsorption of ethanol: E_{01} = 162 kJ/mol;
- Dehydrogenation of the adsorbed-ethanol: E'_{12} = 130 kJ/mol;
- Desorption of acetaldehyde: E'_{20} = 38.5 kJ/mol.

The averaged activation energy of these 3 steps, 110 kJ/mol, is close to the overall activation energy 96 ± 17 kJ/mol determined by Vaidya and Rodrigues.

6. Conclusion

The ethanol steam reforming kinetic data of Vaidya and Rodrigues were analyzed by the rate and yield ratio equations derived from proposed reaction mechanism. A methodology to obtain the general rate equations for cyclic reaction networks was applied to elucidate the kinetics and reaction network analysis of ethanol steam reforming. The derived ethanol rate equation with two lumped kinetic parameters k_a and k_b gave a better fit of ethanol conversion data than that used by Vaidya and Rodrigues who assumed a single rate determining step. The hydrogen yield ratios at different temperatures could be satisfactorily predicted by the yield ratio equation developed in this study. A more detailed analysis of the lumped kinetic parameters at varying reaction temperatures yielded the ethanol adsorption energy on the Ru/Al_2O_3 catalyst to be 162 kJ/mol. The activation energies of dehydration of the adsorbed ethanol and desorption of acetaldehyde were found to be 130 kJ/mol and 38.5 kJ/mol, respectively. No single rate determining step can be assumed to obtain the rate equation that reasonably fit the experimental data. However, some rate controlling steps are water reaction with the adsorbed ethanol, water reaction with the adsorbed acetaldehyde, and CO desorption. Furthermore, for temperature lower than 923 K, the overall reaction is also controlled by desorption of ethanol and desorption of acetaldehyde; for temperature higher than 923 K, the overall reaction is also controlled by the dehydrogenation of the adsorbed ethanol.

Acknowledgements

The Financial supports of this research by Tatung University, Taipei, Taiwan, under the grant B97-C03-022 and Yonglin Foundation to Pei-Jen Lu are gratefully acknowledged.

References

[1] L. Jalowiecki-Duhamel, C. Pirez, M. Capron, F. Dumeignil, E. Payen, Catal. Today 157 (2010) 456.
[2] P. Ciambelli, V. Palma, A. Ruggiero, Appl. Catal. B Environ. 96 (2010) 190.
[3] C.-B. Wang, J.-L. Lee, C.-C. Bi, J.-Y. Siang, J.-Y. Liu, C.-T. Yeh, Catal. Today 146 (2009) 76.
[4] L. Barattini, G. Ramis, C. Resini, G. Busca, M. Sisani, U. Costantino, Chem. Eng. J. 153 (2009) 43.
[5] W. Wang, Y.Q. Wang, Int. J. Energy Res. 32 (2008) 1432.
[6] L. Zhang, W. Li, J. Liu, C. Guo, Y. Wang, J. Zhang, Fuel 88 (2009) 511.
[7] M. Virginie, M. Araque, A.-C. Roger, J.C. Vargas, A. Kiennemann, Catal. Today 138 (2008) 21.
[8] S.M. de Lima, A.M. Silva, I.O. da Cruz, G. Jacobs, B.H. Davis, L.V. Mattos, F.B. Noronha, Catal. Today 138 (2008) 162.
[9] F. Soyal-Baltacioğlu, A.E. Aksoylu, Z.I. Önsan, Catal. Today 138 (2008) 183.
[10] A. Casanovas, C. de Leitenburg, A. Trovarelli, J. Llorca, Catal. Today 138 (2008) 187.
[11] V. Mas, M.L. Dieuzeide, M. Jobbaĭgy, G. Baronetti, N. Amadeo, M. Laborde, Catal. Today 133–135 (2008) 319.
[12] M. Verónica, B. Graciela, A. Norma, L. Miguel, Chem. Eng. J. 38 (2008) 602.
[13] H. Song, L. Zhang, R.B. Watson, D. Braden, U.S. Ozkan, Catal. Today 129 (2007) 346.
[14] M.C. Sánchez-Sánchez, R.M. Navarro, J.L.G. Fierro, Catal. Today 129 (2007) 336.
[15] A. Erdőhelyi, J. Raskó, T. Kecskés, M. Tóth, M. Dömök, K. Baán, Catal. Today 116 (2006) 367.
[16] P.D. Vaidya, A.E. Rodrigues, Ind. Eng. Chem. Res. 45 (2006) 6614.
[17] J. Comas, F. Mariño, M. Laborde, N. Amadeo, Chem. Eng. J. 98 (2004) 61.
[18] D.R. Sahoo, S. Vajpai, S. Patel, K.K. Pant, Chem. Eng. J. 125 (2007) 139.
[19] V. Mas, A.M.L. Bergamini, A.G. Baronetti, N. Amadeo, A.M. Laborde, Top. Catal. 51 (2008) 39.
[20] T.-S. Chen, J.-M. Chern, Chem. Eng. Sci. 57 (2002) 5011.
[21] T.-S. Chen, J.-M. Chern, Chem. Eng. Sci. 58 (2002) 1407.
[22] J.-M. Chern, Ind. Eng. Chem. Res. 39 (2000) 4100.